Soil-Geotextile Pull-Out Interaction Properties: Testing and Interpretation

ILAN JURAN AND CHAO L. CHEN

In this paper are presented a soil-reinforcement load transfer model and a procedure for interpreting pull-out tests on extensible reinforcements. The model combines the constitutive equation of the reinforcement with interaction laws relating the shear stress mobilized at any point of the interface to the soil-reinforcement shear displacement. The main conclusions are (a) extensibility has a major effect on soil-reinforcement interaction; (b) for extensible reinforcement, extrapolation of pull-out test results to reinforcement of different dimensions requires a careful evaluation of the scale effect; and (c) a meaningful interpretation of pull-out test results on geotextiles and geogrids requires an adequate estimation of the in-soil confined properties of the reinforcement and an appropriate soil-geotextile interaction law.

Pull-out interaction properties are fundamental design parameters for reinforced soil systems. The friction interaction between granular soils and quasi-inextensible metallic reinforcing strips has already been extensively investigated by Alimi et al. (*1*), Schlosser and Elias (*2*), Elias (*3*), Guilloux et al. (*4*), Schlosser and Guilloux (*5*), and others. Interpretation of pull-out tests on quasi-inextensible reinforcements provides an apparent friction coefficient that is conventionally defined by the ratio of the interface limit lateral shear stress to the nominal overburden pressure (i.e., the weight of the soil mass above the reinforcement). Compilation of available data from both laboratory and in situ pull-out tests has provided an empirical basis for the development of guidelines for the design of Reinforced Earth structures (*6*).

More recently, the rapid development of a large variety of reinforcing materials and elements has stimulated research on the interaction mechanisms that develop between soil and different types of inclusions such as metallic or plastic geogrids and geotextiles. Pull-out tests have been conducted by McGown (*7*), Gourc et al. (*8*), Ingold (*9*), Jewell (*10*), Rowe et al. (*11*), Johnston (*12*), Shen (*13*), B. Koerner (unpublished internal report No. 1 on Direct Shear/Pull-Out Tests on Geogrids, Drexel University, Philadelphia, Pa., 1986), and others to obtain relevant interaction design parameters (apparent friction coefficient or interface limit lateral shear stress) for different types of geotextiles and geogrids.

Depending on the constitutive material (metal, plastic, woven or nonwoven geotextiles), the geometry and structural aspect of the inclusion (linear strip, ribbed strip, plane reinforcement, geogrid with in-plane or out-of-plane transverse elements, woven or nonwoven geotextiles), the internal grid (or geotextile fiber) spacings, the type of soil and more specifically its grain size and dilatancy properties, different types of load transfer mechanisms can be generated. These mechanisms fundamentally involve four interaction phenomena: (a) lateral friction, plane (membranes) or three dimensional (linear strips, longitudinal elements of geogrids); (b) interlocking (geogrids, geotextiles); (c) passive soil pressure on transverse elements (geogrids, ribbed strips); and (d) the effect of restrained dilatancy on normal stress at the interface (linear inclusions in dilatant granular soils). The relative movement of soil and reinforcement required to bring these phenomena into play can be substantially different. With metallic strip reinforcements, the soil displacement necessary to generate lateral friction at the interfaces is small [millimetric (*1, 2*)]. However, with more extensible reinforcements, or with systems that rely on passive soil pressure on transverse elements, the soil displacement required to generate pull-out resistance can be substantially greater. Therefore, in order to rationally design these systems, it becomes essential to develop a load transfer model that is capable of predicting the pull-out response of the inclusion and specifically its displacements under the applied tension force.

The extensibility of the reinforcement significantly affects the load transfer mechanism. Pull-out tests on geotextiles (*7*) have demonstrated that the interaction between soil and extensible inclusions results in a nonuniform shear displacement distribution that is associated with a shear stress concentration at the front part of the inclusion. Consequently, the concept of a uniformly mobilized interface limit lateral shear stress (or apparent friction coefficient), which is generally used in the design of Reinforced Earth structures with metallic reinforcements, is not adequate for the interpretation of pull-out tests on geogrids and geotextiles. Moreover, as indicated by McGown (*7*), Gourc (*8*), Jewell et al. (*14*), and Koerner, the limit lateral shear stress obtained from the pull-out tests can be significantly different from that determined by direct shear tests with a soil-inclusion interface.

Modeling the load transfer mechanism generated in a pull-out test on extensible inclusions requires appropriate constitutive equations for the soil and the inclusions as well as a rational interaction law to relate the shear stress mobilized at any point of the interface to the soil-rein-

Department of Civil Engineering, Louisiana State University, Baton Rouge, La. 70803.

forcement shear displacement. This interaction law can be obtained from direct shear tests with soil-geotextile interface (*11, 15–17*, and Koerner). The load transfer model should allow for an estimate of the shear stress distribution along the reinforcement and of the front edge displacement caused by the applied pull-out force.

In this paper the authors present an interpretation procedure for pull-out tests on extensible inclusions. This procedure is derived from the "t-z" method, which is commonly used in design of friction piles (*18*). Two interface models are considered in which it is assumed that the interface layer is (a) elastic–perfectly plastic and (b) elasto-plastic with strain hardening and softening during shearing. This interface soil model can be obtained from the results of direct shear tests with a soil-geotextile interface and integrated numerically in the analysis.

To evaluate the proposed test interpretation procedure and the two interface soil models, the results of pull-out tests performed by Juran (*19*) on extensible inclusions (woven polyester and nonwoven geotextile strips) and by Jewell (*10*) on metallic grids were analyzed and compared with numerical test simulations. A parametric study was conducted to assess the effect of the extensibility of the inclusion on its displacement response to the applied pull-out load.

FORMULATION OF SOIL-INCLUSION LOAD TRANSFER MODEL AND PULL-OUT TEST INTERPRETATION PROCEDURE

The principles of discretizing and modeling the load transfer along the reinforcement are illustrated in Figure 1. As indicated previously, the interaction law, which relates the interface shear stress to the soil-reinforcement shear displacement, can be obtained from direct shear tests on a soil sample in which the reinforcement is placed at the level of the failure surface. However, to simplify this analysis, two interface models are considered. These models and their use in test interpretation to obtain the relevant interaction design parameters are presented.

Elastic–Perfectly Plastic Interface Soil Model

The following assumptions are made:

1. The reinforcement is elastic, that is,

$$\varepsilon(x) = \frac{\delta y}{\delta x} = \frac{T(x)}{ES} \tag{1}$$

where

$\varepsilon(x)$ = the elongation of the inclusion at point (x);
$T(x)$ = the tension force at this point;
$y(x)$ = the displacement of the inclusion at point (x);
S = the section area; and
E = the elastic modulus; nonlinear behavior can be considered by introducing an elastic modulus that is a function of the actual strain.

2. The interface layer is elastic–perfectly plastic. The soil-inclusion interaction law can be written as

$$\tau(x) = k \cdot y(x) \quad \text{if } y < \tau_{max}/k \tag{2a}$$

$$\tau(x) = \tau_{max} \quad \text{if } y \geq \tau_{max}/k \tag{2b}$$

where

τ_{max} = $\tan \psi \cdot \gamma h$,
$\tau(x)$ = the shear stress mobilized at point (x),
k = the shear modulus of the interface,
ψ = the soil-inclusion friction angle,
γh = the overburden pressure, and
τ_{max} = the ultimate lateral shear stress at the interface.

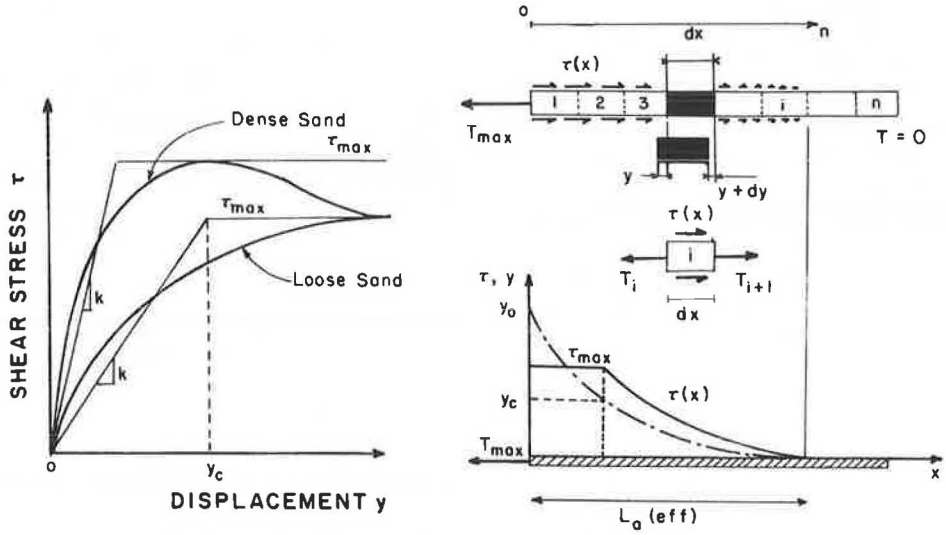

FIGURE 1 Modeling load transfer between soil and extensible inclusion.

The local equilibrium of each segment of the inclusion (Figure 1) implies that

$$\tau(x) = \frac{1}{p}\frac{\delta T}{\delta x} \tag{3}$$

where p is the perimeter ($p = 2b$; b is the width of the inclusion).

By combining Equations 1 and 3, the following differential equation is obtained:

$$\frac{\delta^2 y}{\delta x^2} = \frac{p}{ES}\tau(x) \tag{4}$$

where $\tau(x)$ is given by the interaction law (Equation 2).

The solution of this differential equation for infinitely long inclusion provides the distribution of displacement and tensile forces along the inclusion:

- For $y < y_c = \tau_{max}/k$, the interface is in an elastic range:

$$y = -\frac{\lambda T_0}{ES}e^{-x/\lambda};\ y_0 = -\frac{\lambda T_0}{ES} \tag{5a}$$

$$T(x) = ES\frac{dy}{dx} = T_0 e^{-x/\lambda} \tag{5b}$$

where $\lambda = (ES/KP)^{1/2}$ is a reference "transfer length."

- For $y \geq \tau_{max}/k$, the interface is in a plastic range:

$$y = -\frac{pT_{max}}{ES}\cdot\frac{x^2}{2} + \frac{T_0}{ES}\cdot x + y_0 \tag{5c}$$

$$T(x) = T_0 - p\,\tau_{max}\cdot x \tag{5d}$$

For this case, the front edge displacement of the inclusion (y_0) is calculated by using the compatibility condition at the limit of the elastic and plastic zones, which yields

$y = y_c = -\tau_{max}/k$ and $y_c' = \tau_{max}/(k\lambda)$

Hence, for $y_0 > y_c$,

$$y_0 = \frac{1}{2}y_c\left[1 + \left(\frac{\lambda}{y_c}\right)^2\cdot\left(\frac{T_0}{ES}\right)^2\right] \tag{6}$$

Although the solution is developed for infinitely long inclusions, for the reinforcements commonly used (length l greater than 3λ), the error is negligible.

Figure 2 shows a graphic procedure that can be used for the interpretation of pull-out tests on extensible inclusions to obtain the interaction parameters k and $\tan\psi$. In the plane of $(T/ES)^2$ versus y_0, a linear regression will provide an experimental straight line with

- An initial coordinate at the origin equal to $y_c/2$ and
- A slope equal to $\lambda^2/(2y_c)$.

The soil-reinforcement interface friction angle can then be calculated from

$$\tan\psi = \left(\frac{ES}{p\cdot\gamma h}\right)\cdot\left(\frac{y_c}{\lambda^2}\right) \tag{7}$$

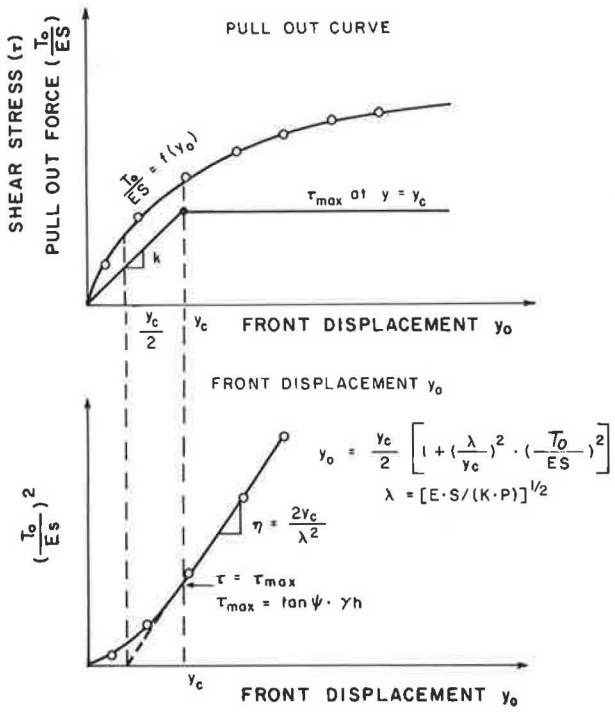

FIGURE 2 Interpretation procedure for pull-out tests on extensible inclusions.

Elastoplastic Strain Hardening Interface Soil Model

To develop a more realistic load transfer model, an elastoplastic constitutive equation is used to simulate the behavior of the interface layer during shearing. This model (*20*), which is implemented by using the finite difference method, allows for the integration of both strain hardening and strain softening in the shear stress–displacement relationship of the soil-inclusion interface. This relation can be written as

$$\frac{\tau(y)}{\sigma_y} = cy\frac{y - a}{(y + b)^2} \tag{8}$$

The constants a, b, and c are determined from the following conditions:

1. The initial shear modulus of the interface layer is equal to

$$\left[\frac{\partial(\tau/\sigma)}{\partial y}\right]_{y\to 0} = \frac{G}{\sigma_y\cdot d}$$

where d is the thickness of the interface layer.

Results of direct shear tests performed by Jewell (*10*) using an x-ray radiographic technique to measure the dis-

placement field in the soil suggest that, in dense unreinforced sand, the thickness of the sheared layer (d) is about 10 to 20 mm.

2. At the peak of the shear displacement–shear stress curve,

$$\frac{\tau}{\sigma_y} = \tan \psi_p$$

where ψ_p is the peak soil-inclusion friction angle.

3. At the residual critical state,

$$\frac{\tau}{\sigma_y} = \tan \psi_r$$

where ψ_r is the residual critical state soil-inclusion friction angle. Hence,

$$a = -4 \frac{\sigma_y d}{G} [\tan^2 \psi_p \cdot J^2]/\tan \psi_r \quad (9a)$$

$$b = 2 \frac{\sigma_y d}{G} [\tan \psi_p \cdot J] \quad (9b)$$

$$c = \tan \psi_r \quad (9c)$$

and

$$J = 1 + [1 - \tan \psi_r/\tan \psi_p]^2 \quad (9d)$$

Coupling the equilibrium equation with the constitutive equations of the inclusion and the interface layer (Equations 4 and 8), the numerical solution for the given boundary conditions of $T_0 = T_p$ (applied pull-out force) and $T_n = 0$ provides the distributions of the displacements and tensile forces along the inclusion. The interaction parameters [$G/(\sigma_y d)$, $\tan \psi_p$, $\tan \psi_r$] are determined using a curve-fitting procedure.

EXPERIMENTAL RESULTS AND NUMERICAL TEST SIMULATIONS

Pull-out tests have been performed on both woven polyester and nonwoven geotextile strips. Figure 3 shows the pull-out box and the instrumentation of the reinforcements. The front edge displacement of the inclusion was measured using both an externally placed graduated scale and potentiometers (change of electrical voltage was calibrated in terms of point displacement). Potentiometers were also placed at different points along the inclusion to provide the displacement distribution under each pull-out load.

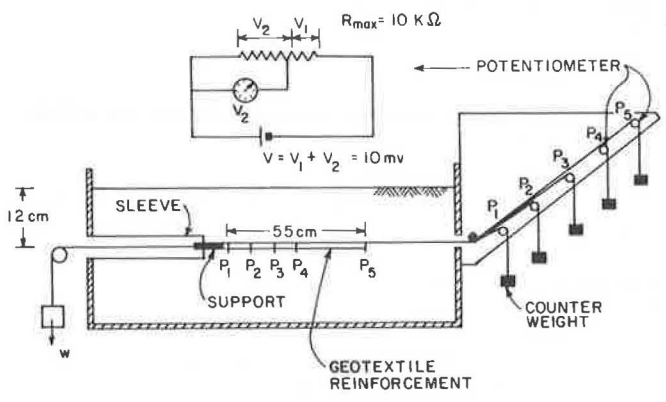

FIGURE 3 Pull-out box and instrumentation.

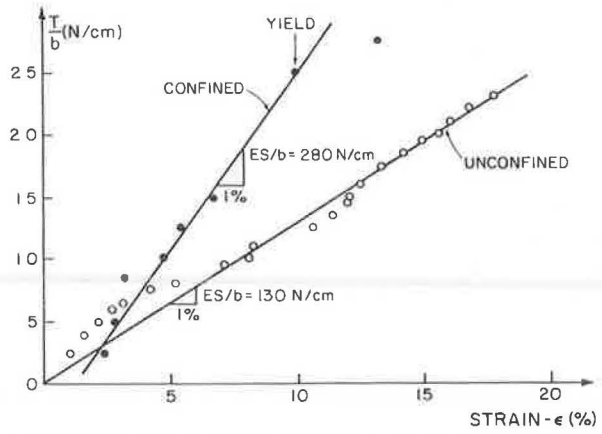

FIGURE 4 Confined and unconfined stress-strain relationship of woven polyester.

Before the pull-out tests, "confined" and "unconfined" extension tests were performed on the reinforcements to determine their in-air and in-soil constitutive equations.

The confined extension tests were performed in the pull-out box under a confining pressure of $\sigma_y = 2$ kPa. The testing procedure consists of applying successive load increments at the front edge of the reinforcement while the rear edge is fixed or simultaneously subjected to the same load increments. A similar load-controlled testing procedure was also used in the pull-out tests with the rear edge of the reinforcement unattached. To avoid any unconfined extension of the front part of the reinforcement during the test, this part was placed between two metal plates. A sleeve was used to minimize the boundary effect, and during the test the inclusion was entirely confined by the surrounding sand.

Figures 4 and 5 show the confined and unconfined stress-

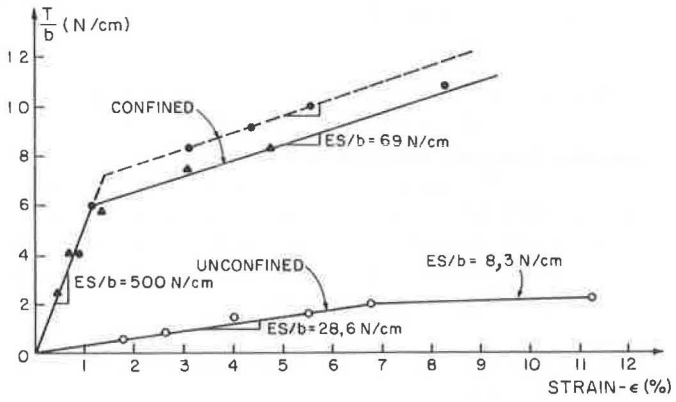

FIGURE 5 Confined and unconfined stress-strain relationship of nonwoven geotextile.

TABLE 1 CONFINED AND UNCONFINED MATERIAL PROPERTIES OF THE REINFORCEMENTS

Reinforcing Material	Unconfined		Confined (σ_y = 2 kPa)		Specimen Length (cm)
	ES/b (N/cm)	T_{cr}/b (N/cm)	*ES/b* (N/cm)	T_{cr}/b (N/cm)	
Woven polyester	130	24	280	28	55
Nonwoven geotextiles	28.6	2.5	500	10	30

NOTE: T_{cr} is the ultimate tensile force at breakage of the sample during a tensile test.

strain relationships of the woven polyester and nonwoven geotextile reinforcements. The related material properties are given in Table 1. These results demonstrate that, for the nonwoven geotextile reinforcement, the confined elastic modulus is about 20 times the unconfined one, and the confined tensile strength is about 4 times the unconfined one.

Figure 6 shows the results of pull-out tests on a woven polyester strip. The distance lag between the front edge displacements measured with the graduated scale and with the potentiometer is most probably due to a local deformation of the metallic wire connecting the measurement point with the potentiometer (such displacement could occur during placement in the soil). It should also be noted that the available instrumentation does not provide accurate displacement readings under relatively low loading levels. However, as shown in Figure 7, the displacement increments measured with the potentiometer correspond fairly well with those measured with the graduated scale. The experimental straight line $y_0 = f([T/ES]^2)$ yields the following interaction parameters:

$\lambda^2/(2y_c) = 3302.88$ mm,
$y_c = 0.7$ mm,
$\lambda = 58$ mm,
$k/\sigma_y = 1.5$, and
$\tan \psi = 1.1$.

Figure 8 shows the variations of the displacements along the inclusion measured under different pull-out loading

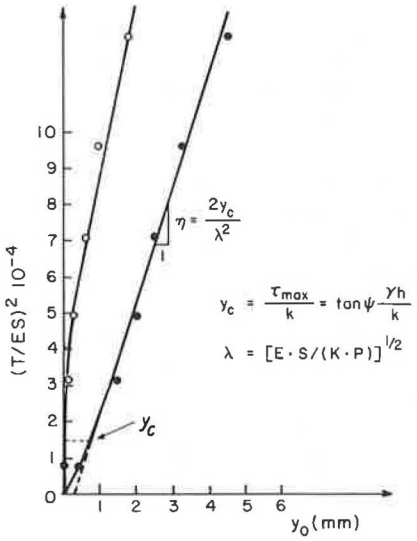

FIGURE 7 Pull-out test on woven polyester: interpretation.

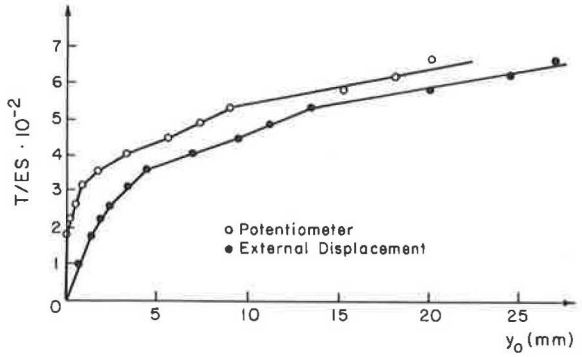

FIGURE 6 Pull-out test on woven polyester: force displacement curve.

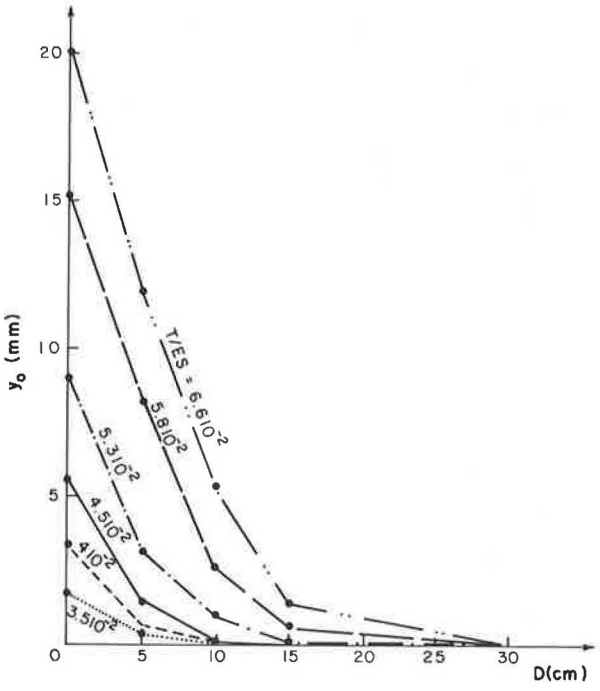

FIGURE 8 Variation of displacements along a woven polyester strip during pull-out test.

levels. Figures 9 and 10 show the results of two pull-out tests on nonwoven geotextile reinforcements. Using the interpretation procedure outlined previously, the following interaction properties are obtained:

$\lambda^2/(2y_c) = 1.5 \times 10^5$ mm,
$y_c = 1$ mm, and
$\lambda = 550$ mm.

The calculated transfer length is greater than the specimen length and therefore the solution derived for infinitely long reinforcement is not applicable.

To evaluate the proposed elastoplastic interface soil model, the experimental results of the pull-out tests performed on the woven polyester and nonwoven geotextile strips as well as those performed by Jewell (*10*) on metallic geogrids were compared with numerical test simulations. Figures 11 and 12 show the experimental and theoretical pull-out curves obtained from tests performed on woven polyester and nonwoven geotextile strips.

For the woven polyester strips, the curve-fitting procedure yields $G/(\sigma_y \cdot d) = 6$ (1/mm) (or $G/\sigma_y = 60$), $\psi_p = 42$ degrees, and $\psi_r = 32$ degrees. Confined elastic modulus is considered in this analysis. These interaction parameters correspond fairly well with the material properties of the Fountainebleau sand used in this study: $G/\sigma_0 = 60$, (σ_0 is the isotropic consolidation pressure), $\phi_p = 38$ to 42 degrees, and $\phi_{cv} = 32$ degrees. It is also of interest to note that the peak soil-reinforcement friction angle obtained using this curve-fitting procedure corresponds to that obtained using the "t-z" method with an elastic–perfectly plastic interface soil model. However, the elastic–perfectly plastic model provides a secant shear modulus (k), which is significantly smaller than the initial shear modulus obtained using the proposed elastoplastic load transfer model.

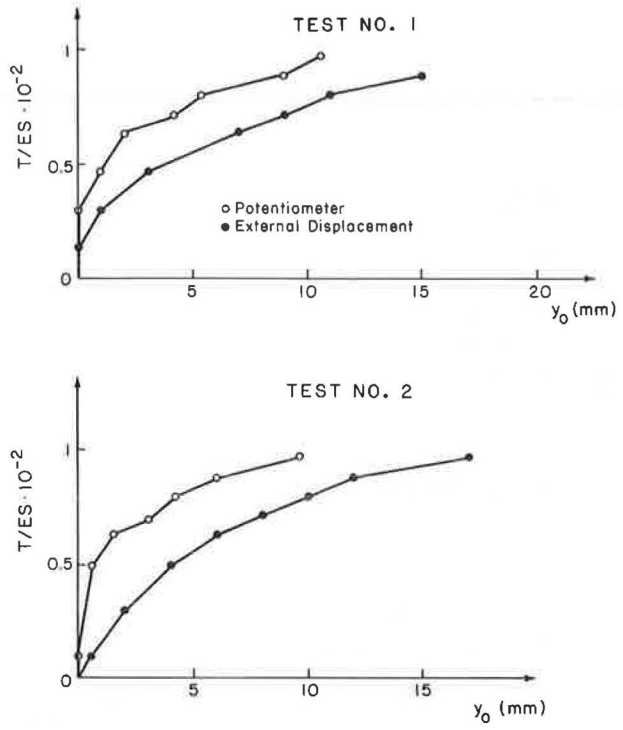

FIGURE 9 Pull-out tests on nonwoven geotextile strips: force-displacement curves.

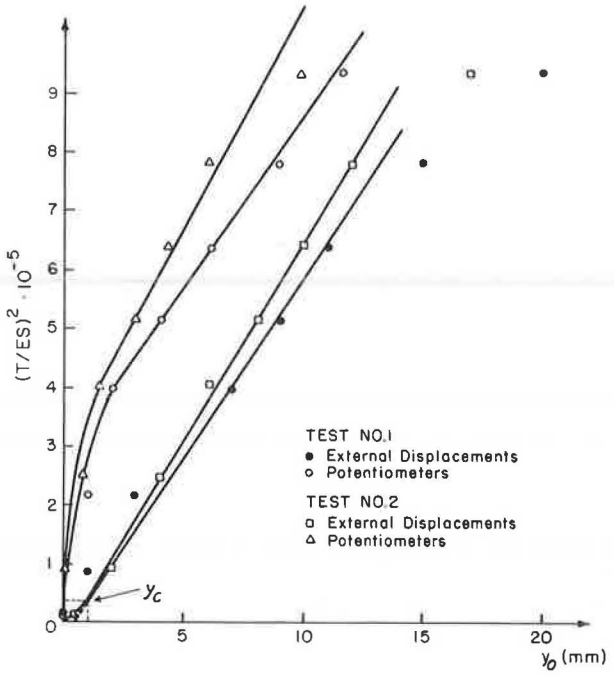

FIGURE 10 Pull-out tests on nonwoven geotextile strips: interpretation.

For the nonwoven geotextile strip, comparison of the theoretical and experimental pull-out curves indicates that using the confined elastic model for test interpretation leads to significantly underestimated displacements. If the unconfined elastic modulus of the reinforcement is used, and assuming that the interface soil properties correspond to the mechanical properties of the Fountainebleau sand, the calculated pull-out curve agrees fairly well with the experimental one.

Figure 13 shows the results of a pull-out test performed

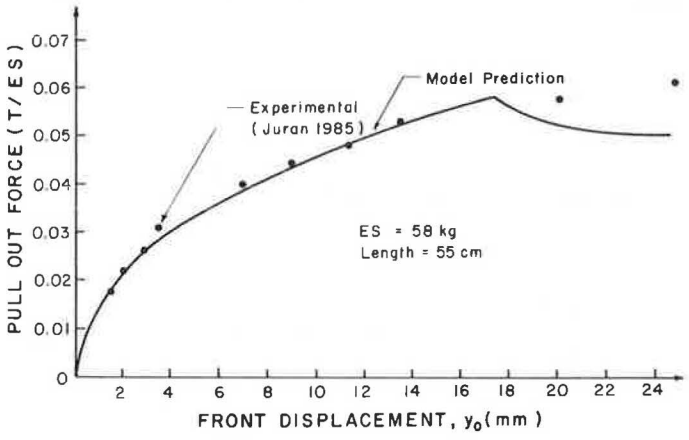

FIGURE 11 Numerical simulation of pull-out test on woven polyester strips.

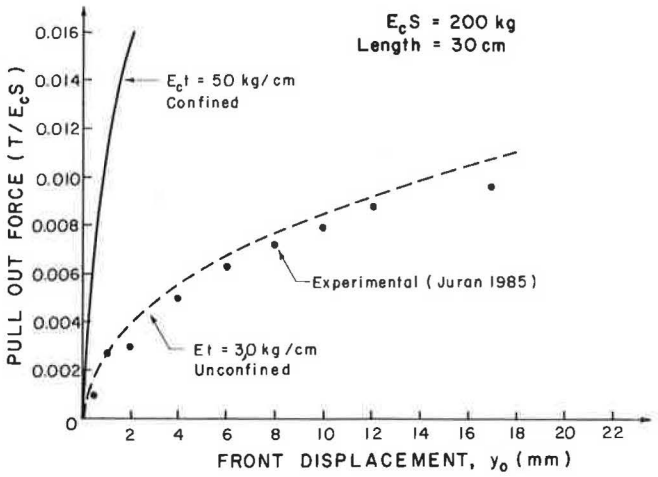

FIGURE 12 Numerical simulation of pull-out test on nonwoven geotextile strips.

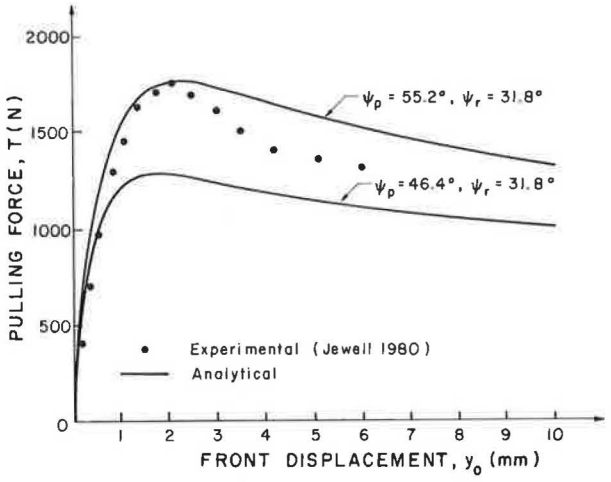

FIGURE 13 Numerical simulation of pull-out test on metallic grid (*10*).

by Jewell (*10*) on metallic grids in Leighton Buzzard sand. The mechanical characteristics of this sand are $G/(\sigma_y d)$ = 4 (1/mm), ϕ_p = 46.4 degrees, and ϕ_{cv} = 31.8 degrees; the applied normal stress is σ_y = 75 kPa. The curve-fitting procedure yields, for interaction parameters, $G/(\sigma_y d)$ = 3 (1/mm), ψ_p = 55.2 degrees, and ψ_r = 31.8 degrees. It can be observed that the peak interface friction angle obtained under the relatively low confining pressure of this test is greater than the peak friction angle of the soil. These results are consistent with those reported by several authors (*9, 12, 14–15*, and Koerner), which indicates that, under low normal stresses, the apparent soil-inclusion interface friction angle obtained from pull-out tests on grids can be significantly greater than the friction angle of the unreinforced soil. The results also indicate that, for this quasi-inextensible reinforcement, the calculated transfer length is significantly greater than the specimen length and therefore the elastic–perfectly plastic solution for an infinitely long reinforcement is not applicable.

Table 2 gives a summary of the interface properties calculated according to the two interaction models and how they compare with soil properties.

EFFECT OF EXTENSIBILITY OF REINFORCEMENT ON PULL-OUT INTERACTION MECHANISM

The proposed soil-inclusion load transfer model can be used to evaluate the effect of the extensibility (or the elastic modulus) of the inclusion on the pull-out curve. Figure 14 shows that pull-out resistance increases with the elastic modulus and that post-peak-strain softening has a significant effect on the soil-inclusion interaction. Figure 15 shows the effect of extensibility on the distribution of displacements along the inclusion, calculated for a loading level approaching the limit pull-out load. Figure 16 shows the effect of extensibility on both the front and the rear edge displacements of the inclusions. The quasi-inextensible inclusion undergoes a quasi-rigid movement, and the shear stress mobilized at the interface is rather uniform. With extensible inclusions (E = 100 MPa), the front edge displacement integrates both the shear displacement of the inclusion and its elongation. The shear stress mobilized at the interface is a function of the soil-inclusion shear displacement and therefore varies along the inclusion. For a loading level approaching the limit pull-out load, the shear

TABLE 2 SOIL AND SOIL-REINFORCEMENT INTERACTION PROPERTIES

	Soil				Interface Model					
					Elastic–Perfectly Plastic			Elastoplastic Strain Hardening		
Reinforcement	G/σ_0 Triaxial	$G/\sigma_y d$ Direct Shear (1/mm)	ϕ_p (degrees)	ϕ_r (degrees)	K/σ_y (1/mm)	y_c (mm)	ψ (degrees)	$G/(\sigma_y d)$ (1/mm)	ψ_p (degrees)	ψ_r (degrees)
Woven polyester geotextile (Juran (*19*))	60	6.0	40–45	32	1.5	0.7	47	6.0	42 (confined *ES*)	32
Nonwoven geotextile (Juran (*19*))	60	6.0	40–45	32	NA	NA	NA	6.0	42 (unconfined *ES*)	32
Metallic grids (Jewell (*10*))	–	4.0	46.4	32	NA	NA	NA	3.0	55	32

NOTE: NA = Not applicable because transfer length exceeds a third of the specimen length ($3\lambda > l$).

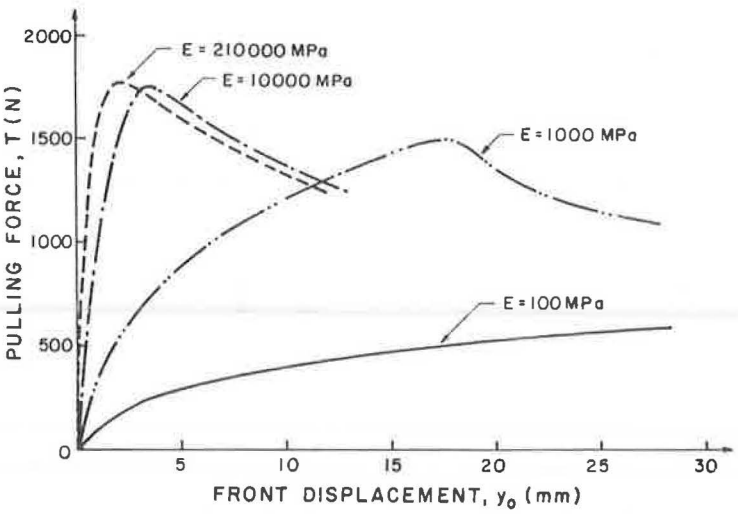

FIGURE 14 Effect of extensibility on pull-out curves.

stress at the front point of the inclusion has attained the residual shear resistance, whereas, at the rear part of the inclusion, the mobilized shear stress is still negligible. At a certain point along the reinforcement, the interface shear stress attains the peak shear resistance.

This nonuniform shear stress distribution demonstrates that the concept of a limit interface shear stress uniformly mobilized along the inclusion (or the apparent friction angle concept), which is currently used in designing with metallic reinforcements, is not adequate for the interpretation of pull-out tests on extensible inclusions to provide relevant interaction design parameters. It also indicates that, in a dense dilating sand, particularly under relatively low normal stresses, the limit interface shear stress obtained from direct shear tests should be superior to that obtained from the pull-out tests. Figure 17 shows the effect of soil density and hence of post-peak-strain softening on the pull-out curve.

EFFECT OF LENGTH OF INCLUSION ON PULL-OUT INTERACTION DESIGN PARAMETERS

The major concern in the engineering interpretation of a pull-out test is scale effect on the relevance of the pull-out

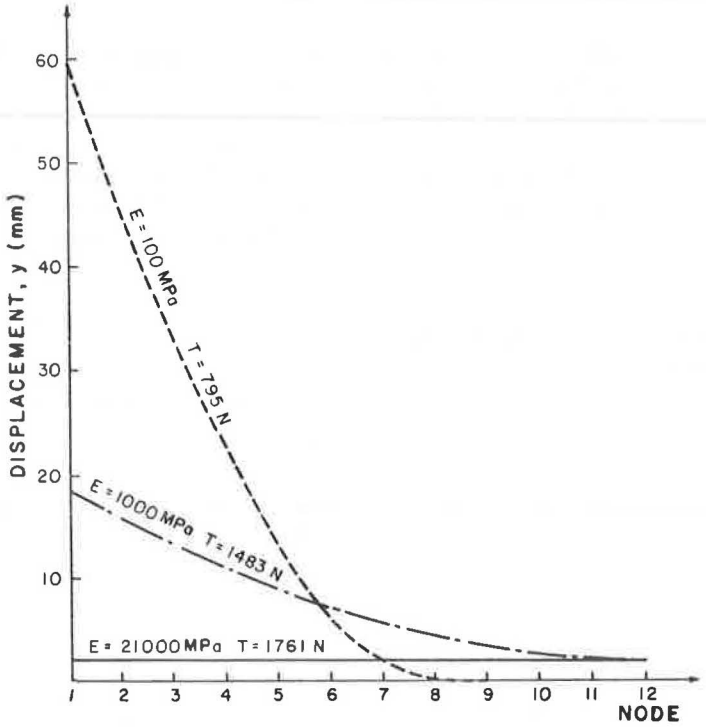

FIGURE 15 Effect of extensibility on distribution of displacements along inclusion.

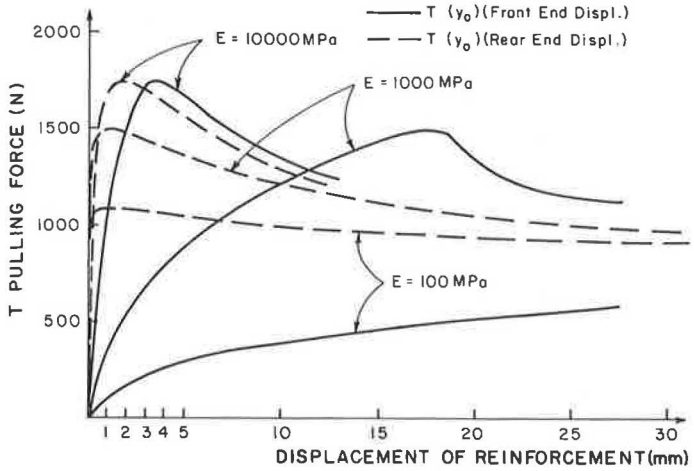

FIGURE 16 Effect of extensibility on front edge and rear edge displacements.

interaction design parameters. Parameters to be used in the design of soil structures with reinforcements of different lengths have to be independent of the dimensions of the sample subjected to a pull-out test.

Figure 18 shows the effect of the length of the reinforcement on the average limit shear stress mobilized at the interfaces at the peak of the pull-out curve. Figure 19 shows the effect of length on peak pull-out displacement. The results of these numerical simulations illustrate that, with quasi-inextensible inclusions, the concept of an apparent friction coefficient, or a uniformly mobilized limit lateral interface shear stress, can be adequately used. The design limit shear stress (or apparent friction coefficient) is independent of the sample dimension, and the results of pull-out tests can therefore be used in the design of actual structures.

With more extensible inclusions, because of nonuniform shear stress distribution, the average limit shear stress mobilized at the peak of the pull-out curve is a function of the sample dimension. Therefore extrapolation of pull-out test results to reinforcements of different lengths requires a careful evaluation of the scale effect.

The numerical simulations also show that as the length of an extensible inclusion increases, the average limit shear stress decreases and approaches a limit value corresponding to the residual interface friction angle. Peak pull-out displacement increases significantly with sample dimension, and consequently a design criterion for allowable pull-out displacement should be considered.

CONCLUSIONS

The main conclusions that can be drawn from this study follow.

1. Soil-inclusion friction interaction depends significantly on the extensibility of the inclusion and the mechanical properties of the interface soil layer.

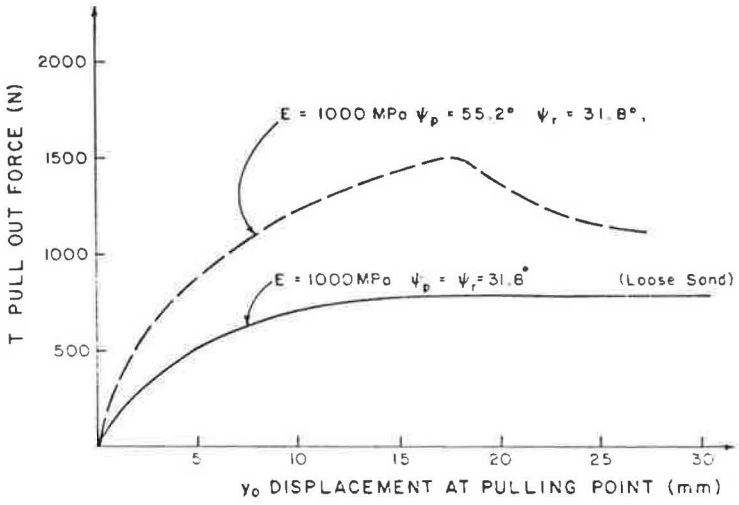

FIGURE 17 Effect of soil density on pull-out curve.

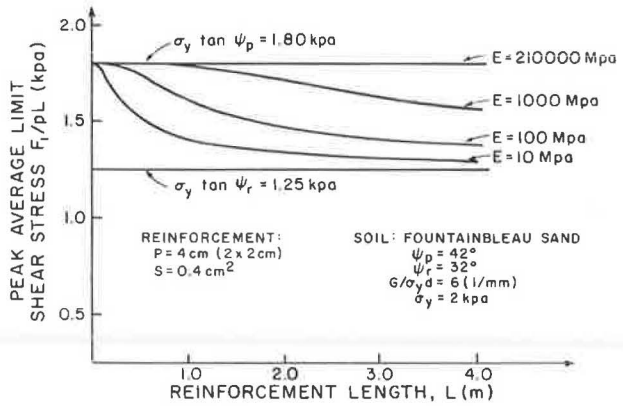

FIGURE 18 Effect of reinforcement length on average limit shear stress.

2. With quasi-inextensible metallic inclusions, the concept of a limit shear stress uniformly mobilized at the interfaces can be adequately used to determine the pull-out resistance of the inclusion. Because the three-dimensional friction interaction between the soil and the inclusion is rather complex, in situ pull-out tests should be performed to provide relevant design parameters.

3. With more extensible inclusions, the elongation of the inclusion during pull-out loading results in a nonuniform shear stress distribution along the reinforcement. The effect of extensibility on the shear stress distribution and the front edge displacements raises major difficulties with regard to the current use of pull-out tests on extensible reinforcements to obtain relevant interaction design parameters. Specifically, because the pull-out resistance is not proportional to the length of the reinforcement, a careful evaluation of the scale effect is required in an extrapolation of pull-out test results to reinforcements of different lengths.

4. A meaningful interpretation of the results of pull-out tests on geotextiles and geogrids requires an appropriate load transfer model. A reliable procedure for the determination of interaction design parameters and the estimation of the pull-out resistance of inclusions therefore necessitates (a) an adequate constitutive equation for the in-soil confined inclusion that is capable of integrating the effect of soil confinement on the mechanical properties of the geofabric and (b) an appropriate interaction law relating the mobilized interface shear stress to the actual soil-reinforcement shear displacement. For geotextiles, this interaction law can be obtained from direct shear tests on a soil-inclusion interface. The pull-out tests, however, allow for an experimental evaluation of the proposed interaction law. They can be efficiently used in situ to determine through a curve-fitting procedure the model-related interaction design parameters.

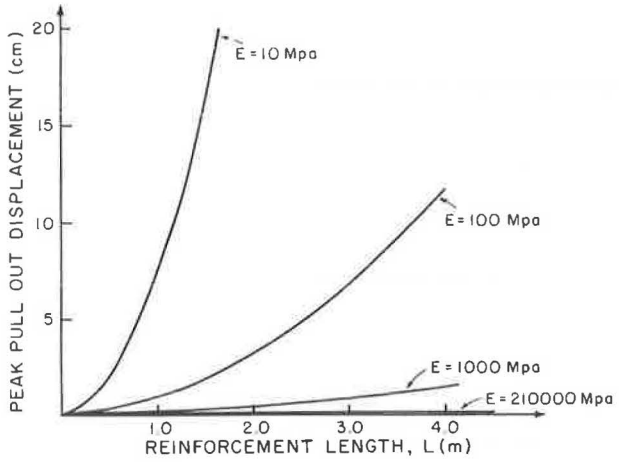

FIGURE 19 Effect of reinforcement length on peak pull-out displacement.

REFERENCES

1. I. Alimi, J. Bacot, P. Lareal, N. T. Long, and F. Schlosser. Etude de l'adherence sol-armatures. *Proc.*, 9th International Conference on Soil Mechanics and Foundation Engineering, Tokyo, Japan, 1977, Vol. 1, pp. 11–14.
2. F. Schlosser and V. Elias. Friction in Reinforced Earth. *Proc.*, Symposium on Earth Reinforcement, ASCE Annual Convention, Pittsburgh, Pa., 1978.
3. V. Elias. Friction in Reinforced Earth Utilizing Fine Grained Backfills. *Proc.*, International Conference on Soil Reinforcement, Paris, France, 1979, pp. 435–438.
4. A. Guilloux, F. Schlosser, and N. T. Long. Etude du frottement sable-armature en laboratoire. *International Conference on Soil Reinforcement*, Paris, France, 1979, Vol. 1, pp. 35–40.
5. F. Schlosser and A. Guilloux. Le frottement dans le renforcement des sols. *Revue Française de Géotechnique*, No. 16, 1981, pp. 65–77.
6. F. Schlosser and P. Segrestin. Dimensionnement des ouvrages en terre armée par la méthode de l'éqilibre local. International Conference on Soil Reinforcement, Paris, France, 1979.
7. A. McGown. The Properties of Nonwoven Fabrics Presently Identified as Being Important in Public Works Applications. *Proc.*, INDEX 78 Congress, European Disposables and Nonwovens Association, 1978, pp. 1.1.1–1.3.1.
8. J. P. Gourc, P. Delmas, and J. P. Giroud. Experiments on Soil Reinforcement with Geotextiles. Presented at ASCE National Convention, Portland, Oreg., 1980.
9. T. S. Ingold. Laboratory Pull-Out Testing of Grid Reinforcements in Sand. *Geotechnical Testing Journal*, Vol. 6, No. 3, 1983, pp. 101–111.
10. R. A. Jewell. *Some Effects of Reinforcement on the Mechanical Behavior of Soil*. Ph.D. dissertation. Cambridge University, Cambridge, England, 1980.
11. R. K. Rowe, S. K. Ho, and D. G. Fisher. Determination of Soil-Geotextile Interface Strength Properties. *Proc.*, 2nd Canadian Symposium on Geotextiles, 1984, pp. 25–34.
12. R. S. Johnston. *Pull-Out Testing of Tensar Geogrids*. M.S. thesis. University of California, Davis, 1985.
13. C. K. Shen. *Final Report on Pull-Out Testing of Tensar SR-2 Geogrids*. Tensar Corporation, Morrow, Ga., 1985.
14. R. A. Jewell, G. W. F. Milligan, R. W. Sarsby, and D. Dubois. Interaction Between Soil and Geogrids. *Symposium on Polymer Grid Reinforcement*, London, England, 1984, pp. 18–30.
15. A. McGown. Reinforced Earth, Discussion to Session 8. *Proc.*, 7th European Conference on Soil Mechanics and Foundation Engineering, Brighton, England, 1979, Vol. 4, pp. 284–287.
16. B. Myles. Assessment of Soil Fabric Friction by Means of

Shear. *Proc.*, 2nd International Conference on Geotextiles, Las Vegas, Nev., 1982, pp. 787–791.
17. S. K. Saxena and J. S. Budiman. Interface Response of Geotextiles. *Proc.*, 11th International Conference on Soil Mechanics and Foundation Engineering, 1985, pp. 1801–1804.
18. H. M. Coyle and L. C. Reese. Load Transfer for Axially Loaded Piles in Clay. *Journal of the Soil Mechanics and Foundation Division*, ASCE, Vol. 92, No. 2, 1966, pp. 1–26.
19. I. Juran. *Internal Research Report on Behavior of Reinforced Soils*. FHWA Project No. DTFH-61-84-C-00073. FHWA, U.S. Department of Transportation, 1985.
20. I. Juran, M. H. Ider, C. L. Chen, and A. Guermazi. Numerical Analysis of the Response of Reinforced Soils to Direct Shearing, Part 2. *International Journal for Numerical and Analytical Methods in Geomechanics*, Vol. 12, No. 2, 1988, pp. 157–171.

Publication of this paper sponsored by Committee on Soil and Rock Properties.